Thermal modulation of fluidic lenses in microgravity

Valeri Frumkin[1] and Rishabh Das[2]

[1]Department of Mathematics, Massachusetts Institute of Technology, Cambridge, MA, 02139 USA

[2]Stuyvesant High School, New York, NY, 10282 USA

December 22, 2021

Abstract

The fluidic shaping method is an exciting new technology that allows to rapidly shape liquids into a wide range of optical topographies with sub-nanometer surface quality. The scale-invariance of the method makes it well suited for for space-based fabrication of large fluidic optics. However, in microgravity, the resulting optical topographies are limited to constant mean curvature surfaces. Here we study how variations in surface tension result in deviations from constant mean curvature topographies, allowing one to introduce optical corrections which would not be obtainable otherwise. Under the assumption of small thermal Peclet number, we derive a differential equation governing the steady-state shape of the liquid surface under the effect of spatially varying surface tension. This equation allows us to formulate an inverse problem of finding the required surface-tension distribution for a desired correction. Lastly, we provide several examples for surface tension distributions yielding required aspheric topographies.

1 Introduction

The majority of space-based imaging systems rely on optical lenses or mirrors for their function. Imaging quality (e.g., resolution or light collection ability) directly depends on the size of the lens/mirror, as well as on physical properties of the optical surface (e.g., surface roughness). Launch constraints limit the size of a single-piece lens/mirror, while deployable telescopes are restricted to multi-segment mirror configurations, resulting in high engineering complexity and significant development time and cost [1]. A notable previous approach to using liquids as the basis for a telescope is spinning a reflecting liquid (typically mercury) round a fixed axis in a gravitational field to produce a parabolic shape [2]. Such telescopes, with a diameter as large as 2.7 meters, were assembled and operated [3], but their main disadvantage is that they rely on continuous and precise spinning of the liquid around the gravitational axis and thus can only be pointed in a single direction [4]. In microgravity, in addition to rotation, this approach requires an external force to replace gravity (e.g., continuous acceleration), making it far less practical.

Recently, a novel method for shaping curable liquids into high-quality optical components, was introduced [5, 6]. The method is based on the injection of a curable lens liquid into a bounding frame

that is submerged in an immiscible immersion liquid environment. If the density of the immersion liquid is set to match that of the lens liquid, gravity is counteracted by buoyancy and the liquid interface takes a shape of a spherical surface. For non-axisymmetric geometries of the bounding frame, the steady-state shape of liquid interface is characterized by a constant mean curvature. Some basic aspheric topographies can also be obtained by allowing the system to deviate slightly from neutral buoyancy, thus allowing gravity to be used as a controllable body force, providing an additional degree of freedom in the design process.

Due to the scale-invariance of the Fluidic Shaping method, it offers a completely different approach for creating space telescopes – launching a volume of liquid that can be compacted into the launcher, and shaping the liquid into a useful optical element in space. Under microgravity conditions the immersion liquid becomes redundant, allowing to apply the new method for extremely heavy optical liquids (e.g., liquid metals [3]) for which no appropriate immersion liquid can be found, preventing their fabrication on Earth.

In orbit, in the absence of body forces, the optical surface can only take shapes of constant mean curvature, which in the case of a ring-shaped bounding surface is a simple spherical cap. However, spherical mirrors/lenses suffer from spherical aberrations which substantially limit their resolution. A potential mechanism for introducing aspheric corrections to the liquid surface is by spatially varying the surface tension of the optical liquid, which can be achieved, for example, by prescribing a non-uniform temperature distribution on the liquid surface. However, thermally induced variation in surface tension result in mass transfer across a liquid interface, known as the thermocapillary effect [7]. In thin liquid films the thermocapillary effect can lead to the deformation of the liquid surface via long wave instability [8]. This deformational instability was recently applied to the fabrication of diffractive optical elements [9]. On larger scales, such as those considered here, thermocapillary convection does not lead to surface deformations and acts mainly as a thermal advection mechanism [10]. Thus, if the thermal diffusion of the reflective liquid is much greater than the thermal advection, the induced thermocapillary flow can be neglected.

Here, we study how in the absence of gravitational acceleration, thermally induced variations in surface tension can modulate the topography of a liquid mirror, allowing to introduce optical corrections to the otherwise constant mean curvature surface. Under the assumption of small thermal Peclet number and weak temperature variations, we derive a governing equation for the steady state shape of the free surface under the effect of spatially non-uniform surface tension distribution. We then proceed to pose the general inverse problem, namely, what will be the surface tension distribution that produces a given surface correction. We show that for the axisymmetric case, the inverse problem can be solved exactly for any sufficiently small aspheric correction to the free surface. Lastly, we discuss how these results can be extended to the general non-axisymmetric topographies, allowing to introduce more general optical corrections.

2 Theory

We consider a configuration where a reflective liquid (e.g. gallium) of volume V is injected into a supporting structure of radius R_0, as is depicted in figure 1. Under microgravity conditions, the liquid surface, $h(r,\theta)$, will take the shape of a spherical cap, corresponding to its minimum energy state [5]. We assume that the temperature of the free surface is prescribed from underneath, by (for example)

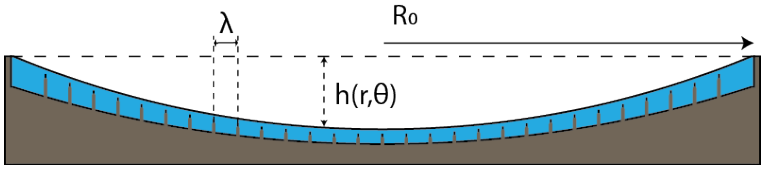

Figure 1: A schematic illustration of the system under consideration: A reflective liquid is deployed into a supporting structure with radius R_0 in microgravity, resulting in a spherical cap shape of the free surface $h(r,\theta)$. The free surface is then heated from bellow by localized heaters separated by a distance λ from one another, resulting in a spatially non-uniform surface tension.

localized heaters separated by a distance λ from one another, leading to a non-uniform distribution of the surface tension

$$\gamma(r,\theta) = \gamma_0 f(r,\theta) = \gamma_0 \left(1 - \gamma_r/\gamma_0 (T(r,\theta) - T_0)\right),$$

where γ_0 is the surface tension at the reference temperature T_0, and $\gamma_r = \frac{\partial \gamma}{\partial T}$.

Under microgravity conditions buoyancy driven flow can be neglected, however, the imposed surface tension gradients will result in thermocapillary flow that will transport liquid across the liquid surface from the hot regions to the cooler ones. For liquids such as gallium, which have high thermal diffusivity and weak temperature dependence of surface tension [11], the rate of thermal diffusion of the liquid is significantly greater than the rate of thermal advection, allowing to establish a stable surface tension gradient with negligible surface velocity. The ratio between these two quantities can be characterized by the Peclet number, $Pe = \frac{\lambda U_0}{\alpha}$, where λ is the characteristic length (in our setup, it is the separation distance between two adjacent heat sources), U_0 is the characteristic flow velocity, and α is the thermal diffusivity of the liquid. For gallium, $\alpha = 3.1 \times 10^{-5}[m^2/s]$, and a typical a typical characteristic thermocapillary velocity is $U_0 = O(10^{-6})[m/s]$ [11, 12], thus separation of $\lambda = 10^{-2}[m]$ is sufficient to achieve $Pe = O(10^{-3}) \ll 1$.

In general, for a driven dissipative system such as the one cosidered here, the rate of change of its free energy is equal to the rate of entropy production, which is proportional to the velocity squared. Thus, considering the small value of the characteristic velocity in our problem, the energy dissipation rate can be neglected, in which case the steady state shape can be found by minimizing the interfacial energy of the liquid. Given a non-uniform distribution of surface tension across the free surface, the free energy functional Π is given by

$$\Pi = \int_0^{2\pi} \int_0^{R_0} E(r,\theta)\, dr\, d\theta,$$

where

$$E(r,\theta) = \left(\gamma \cdot f(r,\theta)\sqrt{1 + h_r^2 + \frac{1}{r^2} h_\theta^2} + \lambda h\right) r.$$

At equilibrium, the first variation of Π must vanish, yielding the Euler-Lagrange equation

$$\frac{\partial E}{\partial h} - \frac{d}{dr}\frac{\partial E}{\partial h_r} - \frac{d}{d\theta}\frac{\partial E}{\partial h_\theta} = 0. \tag{1}$$

The first term in equation (1) is

$$\frac{\partial E}{\partial h} = \lambda \cdot r,$$

the second term is

$$\frac{d}{dr}\frac{\partial E}{\partial h_r} = \frac{\gamma}{r} \cdot r^2 f_r \cdot \frac{h_r}{\sqrt{1 + h_r^2 + \frac{1}{r^2}h_\theta^2}}$$
$$+\frac{\gamma}{r} \cdot f \cdot \frac{rh_r + rh_r^3 + \frac{2}{r}h_r h_\theta^2 + r^2 \cdot h_{rr} + h_{rr}h_\theta^2 - h_r h_\theta h_{r\theta}}{(1 + h_r^2 + \frac{1}{r^2}h_\theta^2)^{3/2}},$$

and the final term is

$$\frac{d}{d\theta}\frac{\partial E}{\partial h_\theta} = \frac{\gamma}{r}\frac{f_\theta h_\theta}{\sqrt{1 + h_r^2 + \frac{1}{r^2}h_\theta^2}} + \frac{\gamma}{r} \cdot f \cdot \frac{h_{\theta\theta} + h_{\theta\theta}h_r^2 - h_r h_\theta h_{r\theta}}{(1 + h_r^2 + \frac{1}{r^2}h_\theta^2)^{3/2}}.$$

Thus, equation (1) can be written as

$$0 = \lambda \cdot r - \frac{\gamma}{r}\left(r^2 \cdot \frac{f_r h_r + f_\theta h_\theta}{\sqrt{1 + h_r^2 + \frac{1}{r^2}h_\theta^2}}\right)$$
$$-\frac{\gamma f}{r} \cdot \left(\frac{rh_r + rh_r^3 + \frac{2}{r}h_r h_\theta^2 + r^2 \cdot h_{rr} + h_{rr}h_\theta^2 - h_r h_\theta h_{r\theta} + h_{\theta\theta} + h_{\theta\theta}h_r^2 - h_r h_\theta h_{r\theta}}{(1 + h_r^2 + \frac{1}{r^2}h_\theta^2)^{3/2}}\right).$$

Multiplying by $\frac{r}{\gamma}$, we get

$$0 = \left(\frac{\lambda}{\gamma}\right)r^2 - \left(\frac{r^2 f_r h_r + f_\theta h_\theta}{\sqrt{1 + h_r^2 + \frac{1}{r^2}h_\theta^2}}\right)$$
$$-f \cdot \left(\frac{r^2 h_{rr}(1 + \frac{1}{r^2}h_\theta^2) + (rh_r + h_{\theta\theta})(1 + h_r^2) - 2h_r h_\theta h_{r\theta} + \frac{2}{r}h_r h_\theta^2}{(1 + h_r^2 + \frac{1}{r^2}h_\theta^2)^{3/2}}\right).$$

2.1 Nondimensionalization

We define the following dimensionless variables and functions:

$$\hat{R} = \frac{r}{R_0},\ \Theta = \theta,\ H(\hat{R}, \Theta) = \frac{h(r,\theta)}{h_0},\ F(\hat{R}, \Theta) = f(r,\theta),\ P = \frac{\lambda R_0^2}{\gamma_0 h_0}$$

where h_0 is the characteristic deformation length scale, and $\varepsilon = \left(\frac{h_0}{R_0}\right)^2 \ll 1$, yielding

$$0 = \frac{P\hat{R}^2}{F} - \left(\frac{\hat{R}^2 F_{\hat{R}} H_{\hat{R}} + F_\Theta H_\Theta}{\sqrt{1 + \varepsilon H_{\hat{R}}^2 + \frac{\varepsilon}{\hat{R}^2}H_\Theta^2}}\right)$$
$$-F \cdot \left(\frac{H_{\hat{R}\hat{R}}(\hat{R}^2 + \varepsilon H_\Theta^2) + (\hat{R}H_{\hat{R}} + H_{\Theta\Theta})(1 + \varepsilon H_{\hat{R}}^2) - 2\varepsilon H_\Theta H_{\hat{R}} H_{\hat{R}\Theta} + \frac{2\varepsilon}{\hat{R}} \cdot H_{\hat{R}} H_\Theta^2}{\left(1 + \varepsilon H_{\hat{R}}^2 + \frac{\varepsilon}{\hat{R}^2}H_\Theta^2\right)^{3/2}}\right).$$

At leading order in ε, the governing equation can be linearized, yielding

$$\frac{P\hat{R}^2}{F} - (\hat{R}^2 F_{\hat{R}} H_{\hat{R}} + F_\Theta H_\Theta) - F \cdot (H_{\hat{R}\hat{R}}\hat{R}^2 + \hat{R}H_{\hat{R}} + H_{\Theta\Theta}) = 0. \tag{2}$$

We will take $P \geq 0$. Substituting $\rho = \hat{R}\sqrt{|P|}$, equation (2) becomes

$$\frac{\rho^2}{F} - (\rho^2 F_\rho H_\rho + F_\Theta H_\Theta) - F \cdot (\rho^2 H_{\rho\rho} + \rho H_\rho + H_{\Theta\Theta}) = 0 \tag{3}$$

where the sign of the first term is determined by the sign of P. Equation (3) describes the steady state configuration of the liquid surface, given a spatial distribution of surface tension. However, it also defines the inverse problem, which is of greater practical importance. The inverse problem can be stated in the following way: what should be the surface tension distribution F, in order to obtain a desired "corrected" surface $H(\rho, \theta)$? Setting $F^2 = G$, equation (3) can be written as

$$\rho^2 - \frac{1}{2}(\rho^2 G_\rho H_\rho + G_\Theta H_\Theta) - G \cdot (\rho^2 H_{\rho\rho} + \rho H_\rho + H_{\Theta\Theta}) = 0 \tag{4}$$

which is a linear, non-homogeneous first-order PDE for G.

2.2 Solving the inverse problem for the axisymmetric case

For most practical purposes the shape of the reflective liquid surface will be that of a spherical cap, therefore it will subject to spherical aberrations. Such aberrations can be corrected by slightly deviating from a spherical surface.

The general description for an aspheric surface is given by

$$z(\rho) = \frac{\rho^2}{R\left(1 + \sqrt{1 - (1+\kappa)\frac{\rho^2}{R^2}}\right)} + \alpha_4\rho^4 + \alpha_6\rho^6 + \cdots,$$

where R is the curvature of the lens, κ is the conic constant, and α_i are higher order corrections. The function $z(\rho)$ itself is known as the sag—the z-component of the displacement of the surface from the vertex, at distance ρ from the axis. For simplicity, we can assume $\kappa = -1$, meaning there are no conic corrections. Thus,

$$z(\rho) = \frac{1}{2R}\rho^2 + \alpha_4\rho^4 + \alpha_6\rho^6 + \cdots.$$

The coefficients α_i has to satisfy the volume constraint, namely,

$$2\pi \int_0^{\sqrt{|P|}} \rho H(\rho)\, d\rho = V \tag{5}$$

where V is the volume of the liquid inside the supporting structure. We then search for a function, $G(\rho)$, that will produce $H(\rho) = H_0(0) - z(\rho)$ as the solution to the axisymmetric version of equation (4), namely,

$$\rho^2 - \frac{1}{2}(\rho^2 G_\rho H_\rho) - G \cdot (\rho^2 H_{\rho\rho} + \rho H_\rho) = 0. \tag{6}$$

Here $H_0(\rho)$ represents the uncorrected surface that is obtained from equation (6) by assuming that

$G = 1$. Solving for H_0 yields

$$H_0(\rho) = \frac{1}{4}\rho^2 + C_1 \ln(\rho) + C_2$$

where C_1 and C_2 are integration constants. Since there cannot be singularities at the origin, $C_1 = 0$, and since H_0 must equal zero at $\rho = \sqrt{|P|}$, we obtain $C_2 = -\frac{1}{4}|P|$. Note that the value of P is also determined by the volume constraint defined in equation (5).

3 Numerical results for axisymmetric surfaces

We proceed to evaluate the required surface tension distribution, $F(\rho)$, in order to obtain a given axisymmetric surface $H(\rho)$. For all cases considered here, the physical parameters were set to be $P = 0.1$, $R = 1.75$, and $V = -0.003927$. Note that the volume is negative as compared to the volume of a flat surface, corresponding to a concave liquid mirror.

Figure 2 shows the cross section of $H_0(\rho)$, the shape of the interface with constant surface tension, along with the full plot of $H_0(\rho)$, which is the cross section rotated about the central axis.

These will serve as reference for other interfaces.

First, we look at $H_1(\rho) = -0.025 + 0.223\rho^2 + 0.783\rho^4 - 5.223\rho^6$, which can be checked to satisfy the necessary conditions previously mentioned. The cross section of this interface along with the full plot are shown in figure 3. The interface this forms has a very similar shape to $H_0(\rho)$, but there are small perturbations, which can be seen in figure 4. We can then numerically solve for the desired surface tension distribution, which can be seen in figure 5.

As an additional example, we will take $H_2(\rho) = -0.025 + 0.257\rho^2 - 4.285\rho^6 + 35.714\rho^8$, which can also be checked to satisfy the necessary conditions previously mentioned. The cross section of this interface along with the full plot are shown in figure 6. The difference between $H(\rho)$ and $H_0(\rho)$ can be seen in figure 7. We can then numerically solve for the desired surface tension distribution, which can be seen in figure 8.

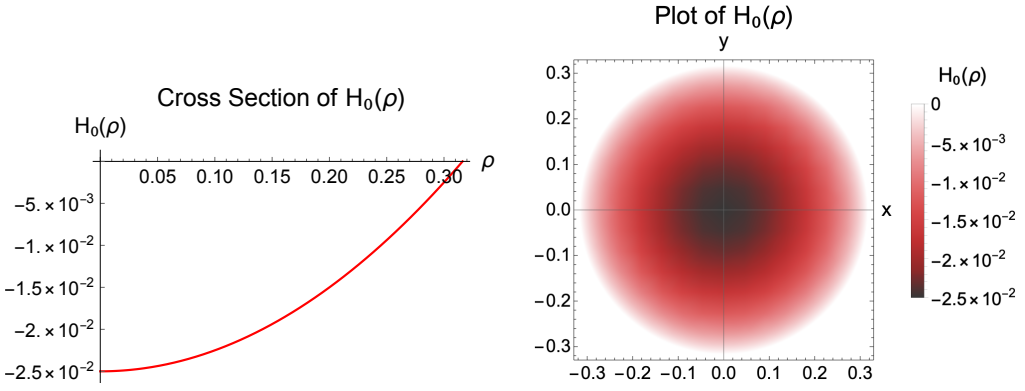

Figure 2: Cross section (left) and top view color map (right) of the uncorrected surface profile $H_0(\rho)$, corresponding to constant surface tension.

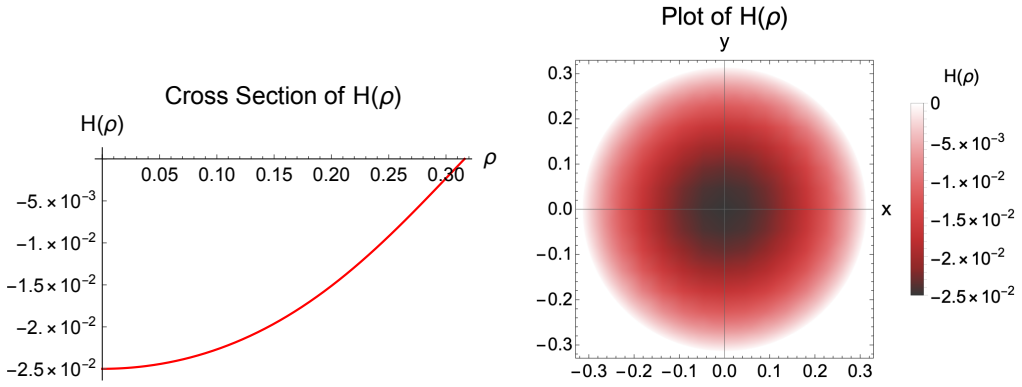

Figure 3: Cross section (left) and top view color map (right) of the aspheric surface $H_1(\rho)$.

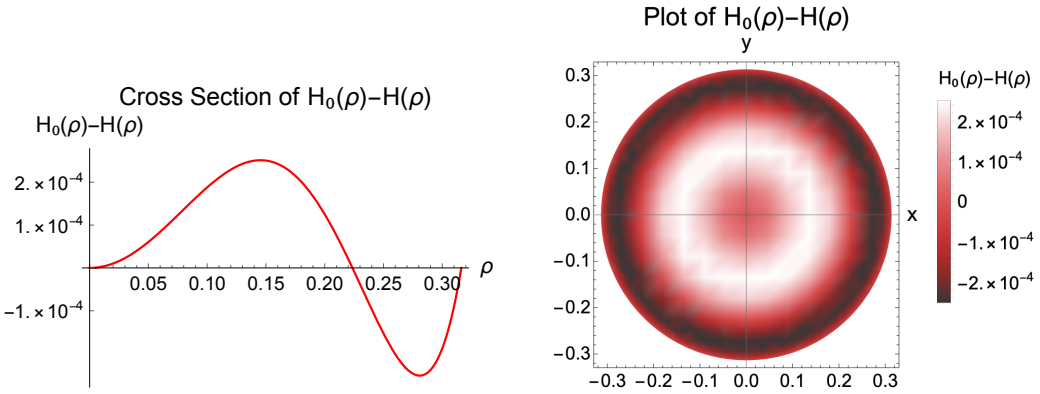

Figure 4: Cross section (left) and top view color map (right) of the difference $H_0(\rho) - H_1(\rho)$, showing the added correction to H_0.

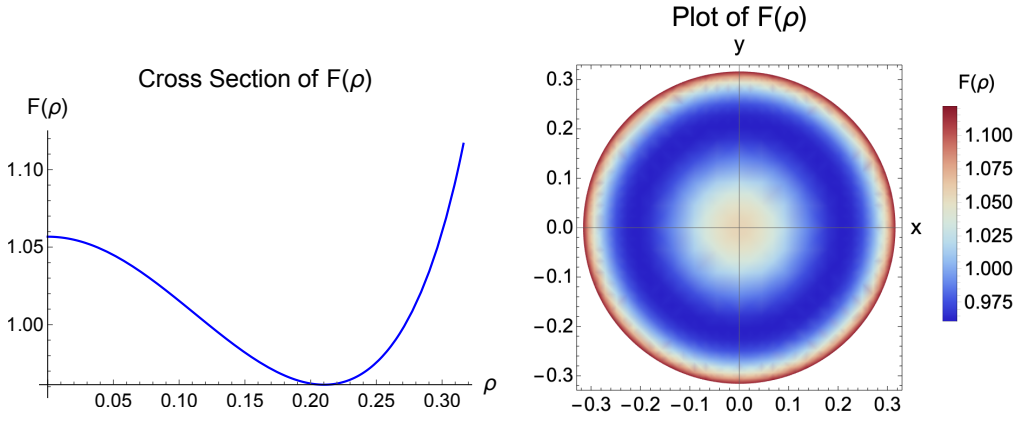

Figure 5: Cross section (left) and top view color map (right) of the surface tension distribution $F(\rho)$, corresponding to the corrected surface $H_1(\rho)$, as calculated from Eq. (6).

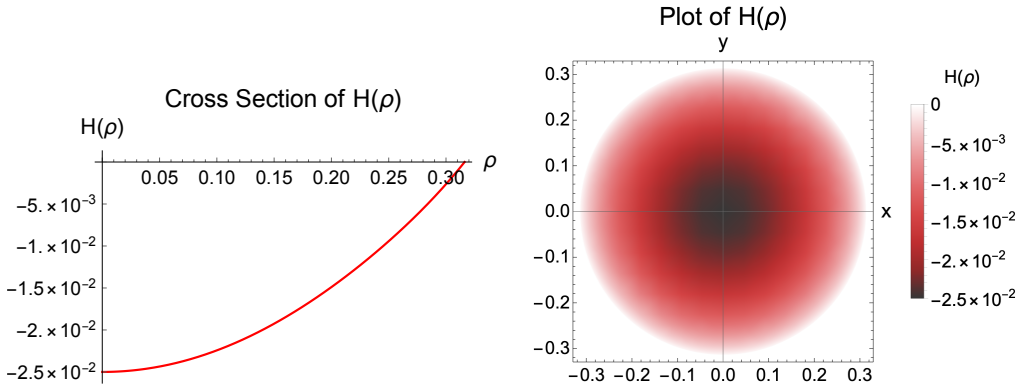

Figure 6: Cross section (left) and top view color map (right) of the aspheric surface $H_2(\rho)$.

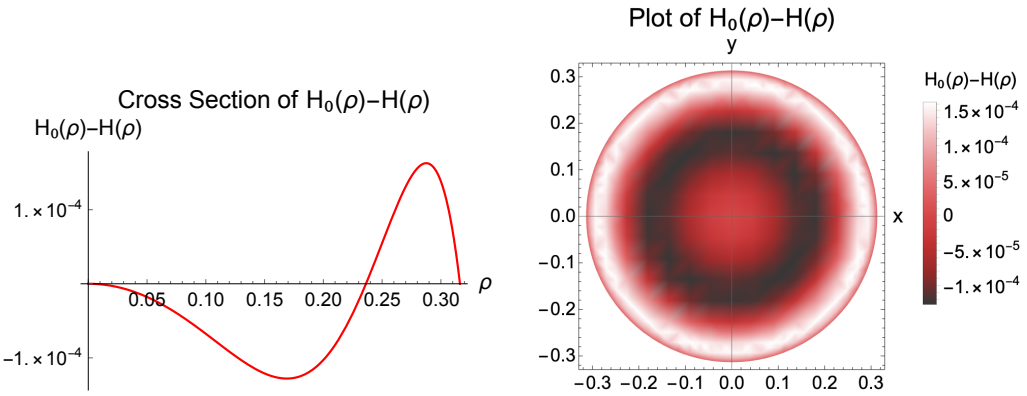

Figure 7: Cross section (left) and top view color map (right) of the difference $H_0(\rho) - H_2(\rho)$, showing the added correction to H_0.

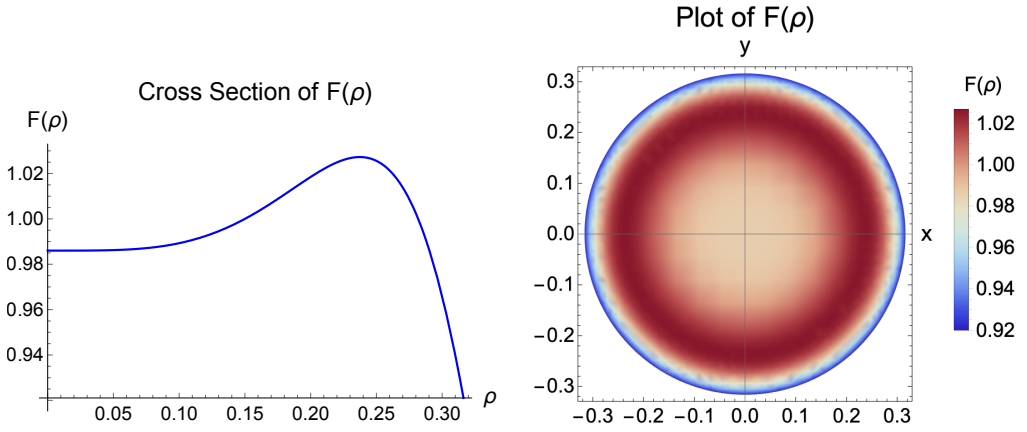

Figure 8: Cross section (left) and top view color map (right) of the surface tension distribution $F(\rho)$, corresponding to the corrected surface $H_2(\rho)$, as calculated from Eq. (6).

4 Discussion

In this work we have demonstrated how a liquid surface can be modulated by means of thermally varying its surface tension. Under the assumption of small Peclet number, we derived a steady state surface equation connecting a non-uniform distribution of surface tension to the resulted profile of the liquid surface. We showed how this equation can be used to solve the inverse problem, namely, given a targeted surface profile, what is the required surface tension distribution required to achieve it. Here we focused on axisymmetric, reflective concave surfaces (i.e., liquid mirrors), for which we have demonstrated how aspheric correction can be introduced to an otherwise spherical surface. However, the model derived here is valid for non-axisymmetric surfaces as well. Thus, a natural extension of this work would be to consider general optical correction to spherical surfaces, which can be represented, for example, by a sum of Zernike polynomials [13], potentially allowing the use freeform optical designs in future fluidic space telescopes.

5 Acknowledgements

The authors would like to thank MIT's PRIMES-USA program for the opportunity to collaborate together. They would also like to thank Kent Vashaw for reviewing the paper and providing helpful comments.

References

[1] Feenix Y. Pan, James H. Burge, Rene Zehnder, and Yanqui Wang. Fabrication and alignment issues for segmented mirror telescopes. *Applied Optics*, 43(13):2632–2642, May 2004. Publisher: Optical Society of America.

[2] Paul Hickson, Gordon A. H. Walker, Ermanno F. Borra, and Remi Cabanac. 2.7-m liquid-mirror telescope. In *Advanced Technology Optical Telescopes V*, volume 2199, pages 922–927. International Society for Optics and Photonics, June 1994.

[3] Ermanno F. Borra. *1 Liquid Mirror Telescopes: A Review*. 1997.

[4] V. P. Vasilev. On the problem of using liquid mirrors in astronomy. *Astronomicheskii Zhurnal*, 62:598–601, June 1985.

[5] Valeri Frumkin and Moran Bercovici. Fluidic shaping of optical components. *Flow*, 1, 2021. Publisher: Cambridge University Press.

[6] Mor Elgarisi, Valeri Frumkin, Omer Luria, and Moran Bercovici. Fabrication of freeform optical components by fluidic shaping. *Optica*, 8(11):1501–1506, November 2021. Publisher: Optical Society of America.

[7] S. H. Davis. Thermocapillary Instabilities. *Annual Review of Fluid Mechanics*, 19(1):403–435, 1987.

[8] A. Oron, S. H. Davis, and S. G. Bankoff. Long-scale evolution of thin liquid films. *Reviews of Modern Physics*, 69(3):931–980, July 1997.

[9] Ran Eshel, Valeri Frumkin, Matan Nice, Omer Luria, Boris Ferdman, Nadav Opatovski, Khaled Gommed, Maxim Shusteff, Yoav Shechtman, and Moran Bercovici. Fabrication of diffractive optical elements by programmable thermocapillary shaping of thin liquid films. *arXiv:2109.00158 [physics]*, August 2021. arXiv: 2109.00158.

[10] Y. Kamotani, S. Ostrach, and A. Pline. A Thermocapillary Convection Experiment in Microgravity. *Journal of Heat Transfer*, 117(3):611–618, August 1995.

[11] S. C. Hardy. The surface tension of liquid gallium. *Journal of Crystal Growth*, 71(3):602–606, May 1985.

[12] K. E. Spells. The determination of the viscosity of liquid gallium over an extended nrange of temperature. *Proceedings of the Physical Society*, 48(2):299–311, March 1936. Publisher: IOP Publishing.

[13] Jim Schwiegerling. Review of Zernike polynomials and their use in describing the impact of misalignment in optical systems. In *Optical System Alignment, Tolerancing, and Verification XI*, volume 10377, pages 74–81. SPIE, August 2017.